

# **Interfacial Characterisation of Sol-Gel Derived Coatings of Hydroxyapatite and Zirconia Thin Films with Anodised Titanium Substrates**

A THESIS SUBMITTED IN FULFILMENT OF THE REQUIREMENTS FOR THE  
DEGREE OF DOCTOR OF PHILOSOPHY

BY

**Richard Roest**

B.Sc. M.Sc. (UTS)



UNIVERSITY OF TECHNOLOGY, SYDNEY

November 2008

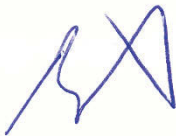
© RICHARD ROEST 2008

## **CERTIFICATE OF AUTHORSHIP/ORIGINALITY**

I certify that this thesis has not previously been submitted for a degree nor has it been submitted as part of the requirements for a degree except as fully acknowledged within the text.

I also certify that the thesis has been written by me. Any help that I have received in my research work and the preparation of the thesis itself has been acknowledged. In addition, I certify that all information sources and literature used are indicated in the thesis.

Signature of Candidate



---

## ABSTRACT

The anodisation of titanium involves the formation of a thin, compact oxide layer, which improves the wettability of the oxide film. This process involves the conversion of the rutile structure of the original titanium oxide into a mixed rutile and crystalline anatase structure. An understanding of the anodised structure and how it influences the bonding properties of the sol-gel coating of hydroxyapatite (HAp) and zirconia is the main focus of this research project.

The titanium samples were anodised in a mixed phosphoric acid ( $\text{H}_3\text{PO}_4$ ) sulphuric acid ( $\text{H}_2\text{SO}_4$ ) solution. The samples were also anodised at three different voltages, 25V, 50V and 75 Volts for 30 minutes. Both anodised and original titanium samples were spin coated with alkoxide-derived hydroxyapatite and zirconia sol-gel coatings and examined using X-ray diffraction and scanning electron microscopy. By controlling the oxide layer formed on the titanium substrates, its thickness and the amount of anatase formed in the mixed oxide layer as well as the oxide films porosity enabled the preparation of an oxide film surface that yielded the optimum conditions for coating with the sol gel solutions.

The diffusion theory can be seen to operating in the coating of the sol gel films through interdiffusion of the sol gel coating into the titanium oxide layer, with zirconium ions detected in the titanium oxide layer up to a depth of 75 microns and in the case of the hydroxyapatite sol gel coating phosphorus and calcium was detected in the titanium oxide layer.

The adhesion of the sol gel coated samples was tested using a micro-adhesion tester and the zirconia samples were further tested on an Ortho-pod tribological tester to determine the wear properties. The results show a significant improvement in interfacial energy of the hydroxyapatite films on the Ti6Al4V substrates over the C.P. titanium substrates with the anodised 25 volt and 50 volt Ti6Al4V substrate yielding values of 12.1 and 12.8 J/m<sup>2</sup> compared with values of less than 2 J/m<sup>2</sup> for the C.P. titanium samples.

Experimentation also shows that for both C.P. Titanium and Ti6Al4V substrates the 25 and 50 volt anodised samples for the crack free zirconia have interface toughness values in excess of 1.5 MPa.m<sup>1/2</sup> in addition to them the Ti6Al4V substrate also is in excess of 1.5 MPa.m<sup>1/2</sup> indicating that these samples all possess good interface toughness values while the other substrates have toughness values half the previously mentioned samples of about 0.75 MPa.m<sup>1/2</sup>.

The zirconia solution used was modified with 1- Butanol to reduce the viscosity of the zirconia sol gel to 10 -12 centipoise and this lead to the formation of a crack free zirconia coating of 100 nm thickness when spin coated, also the tetragonal polymorph was found on all substrates tested with X-ray diffraction.

Tribological results on the zirconia-coated titanium samples, both anodised and control, showed the titanium samples yielded better wear-resistance properties than the double coated samples. The 50 volt anodised titanium samples yielded the best wear resistance of all samples tested after 500,000 cycles on the Ortho-pod machine in water.

## **Acknowledgements**

I am deeply indebted to a number of people for their help and guidance throughout the duration of this degree. In particular, I would like to express my deepest gratitude to my supervisor, Associate Professor Besim Ben-Nissan for the guidance, encouragement, expertise and friendship he has given during this degree.

Special thanks to Dr Greg Heness, Dr Norman Booth, Alex Rubel and Jules Guerbois for their support and assistance; their time and enthusiasm are greatly appreciated.

I would also like to offer a special thank you to the following people for their assistance with this research study:

- Associate Professor Matthew Phillips, Dr Richard Wuhler, Mark Berkahn and Ms Katie McBean from the Micro structural Analysis Unit of UTS, whose help and encouragement with the SEM and XRD analysis were greatly appreciated.
- Associate Professor Alan W. Eberhardt and Carrie Stewart from the University of Alabama, who assisted with the tribological testing of my samples.

I would also like to acknowledge the support of the Australian Institute for Nuclear Science and Engineering (AINSE) for giving me a Postgraduate Research Award which provided access to a wide range of facilities at the Lucas Heights site, and I would also like to acknowledge the support of the Australian Nuclear Science and Technology Organisation (ANSTO) Materials Engineering Division.

I would also like to give special thanks to Dr Bruno Latella from the Materials Engineering Division of ANSTO who helped conduct the micro-adhesion testing and provided endless assistance and mentoring during the project in addition to his friendship and guidance which made the journey towards completing my thesis more enjoyable.

Finally, a special thanks to my family and close friends for their support and confidence during this project.

# TABLE OF CONTENTS

Authorship Certificate .....	i
ABSTRACT .....	II
Acknowledgements .....	iv
TABLE OF CONTENTS .....	VI
LIST OF TABLES .....	X
LIST OF FIGURES AND ILLUSTRATIONS .....	XI
APPENDIX .....	XV
LIST OF SYMBOLS, ABBREVIATIONS AND NOMENCLATURE .....	XVI
PUBLICATION LIST .....	XVII
CHAPTER 1 - INTRODUCTION .....	1
1.1 Background .....	1
1.2 Thesis Structure .....	2
1.3 Statement of Study Aims .....	3
CHAPTER 2 – TITANIUM SUBSTRATES AND ANODISING .....	4
2.1 Titanium .....	4
2.2 Titanium Anodising .....	5
2.3 Formation Mechanism of Anodic Oxide Films .....	8
2.4 Growth Modes for Anodic Oxide Films .....	9
2.5 Anodising Surface Roughness .....	14
2.6 Titanium Corrosion Resistance .....	15
2.6.1 General Corrosion Resistance .....	15
2.7 Anodising Set-up and Processes .....	16
2.8 Anodising Solutions .....	17
2.9 Anodised Samples .....	18
CHAPTER 3 - SOL GEL PROCESS – HYDROXYAPATITE AND ZIRCONIA COATINGS .....	24
3.1 Hydroxyapatite .....	24
3.1.1 Hydroxyapatite Production Methods .....	25

3.2 Hydroxyapatite Experimental Method.....	26
3.2.1 Hydroxyapatite Coating Procedure .....	27
3.3 Zirconia.....	29
3.3.1 Zirconia Coatings.....	30
3.4 Zirconia Experimental Procedure .....	31
3.5 Zirconia Sol Gel Discussion.....	33
CHAPTER 4 – BIOCOMPATIBLE INTERFACES .....	38
4.1 Cellular Adhesion and Biocompatibility .....	38
4.2 Implant Interface design.....	39
4.3 Osteoblasts Adhesion .....	40
4.4 Osteoblast Cell Culturing and Bio-Assays.....	40
4.4.1 Experimental method .....	41
4.5 Results and Discussion .....	42
4.5.1 Cell Growth and Cytotoxicity .....	45
4.6 Cell growth Conclusions .....	50
CHAPTER 5 – INTERFACE ANALYSIS WITH SIMS .....	52
5.1 Secondary Mass ion Spectrometry (SIMS) .....	52
5.1.1 Secondary Mass ion Spectrometry (SIMS) method.....	52
5.2 Results and Discussion .....	53
5.3 SIMS Interface Conclusions .....	62
CHAPTER 6 – XRD ANALYSIS OF THIN FILMS .....	64
6.1 Titanium X-Ray Diffraction (XRD) .....	64
6.1.1 XRD Analysis of Titanium Samples .....	64
6.2 Titanium X-Ray Diffraction - Experimental Results .....	65
6.3 Hydroxyapatite Sol Gel Coatings XRD Analysis .....	68
6.4 Zirconia Sol Gel Coatings XRD Analysis .....	71
CHAPTER 7 – THIN FILM ADHESION AND SURFACE PROPERTIES .....	74
7.1 Coatings Film Adhesion.....	74
7.2 Mechanical Theory .....	75
7.3 Chemical Bond Theory .....	76



7.4	Electrostatic Theory .....	77
7.5	Diffusion Theory .....	77
7.6	Mechanics of Adhesion.....	77
7.6.1	Wettability and Surface Energetics .....	78
7.6.2	Interfacial Thermodynamics .....	78
7.6.3	Contact Angle .....	79
7.6.4	Contact Angle Discussion .....	80
7.7	Scanning Electron Microscopy (SEM).....	82
7.8	Surface roughness .....	82
7.8.1	Surface Roughness Discussion .....	83
CHAPTER 8 – MECHANICAL MICRO ADHESION AND NANO HARDNESS TESTING .....		86
8.1	Mechanical Sample Preparation.....	86
8.2	Adhesion Test Methods .....	88
8.3	Micro-Adhesion Testing of Thin Films .....	89
8.4	Mechanical Properties.....	90
8.4.1	Critical Stress for Cracking .....	91
8.4.2	Fracture Energy of Film .....	91
8.4.3	Fracture Film Toughness.....	92
8.5	Dog-Bone Samples used in Micro-Adhesion Testing.....	92
8.5.1	Micro-Adhesion Testing Method.....	93
8.6	Micro-Adhesion Testing Results.....	95
8.6.1	Micro-Adhesion Discussion .....	96
8.7	Micro-Adhesion Conclusions.....	108
8.8	Nano-Indentation Testing.....	110
CHAPTER 9 – TRIBOLOGICAL PROPERTIES.....		114
9.0	Tribology .....	114
9.1	Friction.....	114
9.2	Ceramics Wear .....	115
9.3	Titanium – Friction Properties .....	116
9.4	Tribology Testing .....	117

9.4.1	Tribology Testing Procedure .....	118
9.4.2	Frictional Wear Testing .....	118
9.5	Statistical Analysis .....	120
9.6	Results and Discussion .....	121
CHAPTER 10 – CONCLUSION .....		126
BIBLIOGRAPHY .....		132
APPENDIX .....		145

## LIST OF TABLES

Table 4.1	Properties of the Osteoblast Phenotype From Cell Biology of Bone by Martin et al. [133].....	38
Table 4.2	Osteocalcin Concentration Data over 14 day Period .....	42
Table 4.3	Osteocalcin Concentration Data over 14 day Period with Standards and Blanks .....	43
Table 4.4	Saos raw data produced with Propium Iodide.....	47
Table 4.5	Saos raw data averages produced with Propium iodide.....	47
Table 4.6	Mg63 raw data produced with Propium Iodide.....	48
Table 4.7	Mg63 raw data averages produced with Propium iodide.....	48
Table 7.1	Contact Angle measured using drop shape analysis with 15 $\mu$ L drop .....	81
Table 7.2	Surface Roughness of Titanium Samples measured using KLA Tencor Alpha-Step IQ Surface Profiler .....	84
Table 7.3	Surface Roughness of Sol Gel Coated Titanium Samples measured using KLA Tencor Alpha-Step IQ Surface Profiler. ....	85
Table 8.1	Ti6AL4V Sample polishing method using STRUERS Autopolisher .....	87
Table 8.2	C.P Titanium Sample polishing method using STRUERS Autopolisher .....	87
Table 9.1	Tribology Testing Matrixes for Titanium Samples with Cracked Zirconia Coating.....	117
Table 9.2	Wear tables for zirconia coated titanium samples and list showing samples used in testing .....	122

## LIST OF FIGURES AND ILLUSTRATIONS

Figure 2.1	Illustration of titanium anodising cell before current is applied, based on a Christiane Jung presentation. [56].....	11
Figure 2.2	Start of the anodised titanium oxide layer formation showing the oxygen ions moving into the titanium oxide layer. [56].....	12
Figure 2.3	Final layer formation after the titanium oxide is finished growing. [56] .....	12
Figure 2.4	Ra Surface roughness chart of both C.P. Titanium and Ti6Al4V alloy anodised at 25 Volts. ....	14
Figure 2.5	Titanium Anodising rack with anodic oxide film evident after use .....	18
Figure 2.6	Heat-treated (550°C) samples, showing homogeneity of anodised samples, in concentrated solutions. ....	20
Figure 2.7	Ti6Al4V sample anodised at 25V .....	21
Figure 2.8	C.P. Titanium sample anodised at 25V .....	21
Figure 2.9	C.P. Titanium sample anodised at 50V .....	22
Figure 2.10	Ti6Al4V sample anodised at 50V .....	22
Figure 2.11	C.P. Titanium sample anodised at 75V .....	23
Figure 2.12	Ti6Al4V sample anodised at 75V .....	23
Figure 3.1	Hydroxyapatite sol gel flowchart .....	28
Figure 3.2	Zirconia sol gel flowchart .....	32
Figure 3.3	SEM of 200nm thick zirconia sol gel coating on 75V anodised C.P. titanium showing cracking in coating. ....	34
Figure 3.4	SEM of 200nm thick zirconia sol gel coating on 75V anodised C.P. titanium showing cracking in coating. ....	35
Figure 3.5	Optical micrograph of 100nm thick zirconia sol gel coating on 75V anodised C.P. titanium showing crack free coating. ....	36
Figure 3.6	SEM of 200nm thick zirconia sol gel coating on C.P. titanium substrate showing reduced cracking in zirconia coating with reduced viscosity (20CPS) .....	37
Figure 3.7	SEM of 200nm thick zirconia sol gel coating on C.P. titanium substrate showing no cracking in zirconia coating with final viscosity (10-12 CPS). ....	37

Figure 4.1	Osteocalcin standard curve over 14 day period .....	44
Figure 4.2	Osteocalcin production over 14 day period .....	44
Figure 4.3	Saos standard curve produced with Propium Iodide .....	46
Figure 4.4	Mg 63 standard curve produced with Propium Iodide .....	46
Figure 4.5	Mg63 cell numbers produced with Propium iodide.....	49
Figure 4.6	Saos cell numbers produced with Propium iodide.....	49
Figure 5.1	Ti6Al4V Alloy with zirconia coating showing sputtered area through zirconia coating with the scale at 100 microns. ....	53
Figure 5.2	Interior of SIMS sputtered area on Ti6Al4V alloy coated with zirconia showing alpha and beta grains. ....	54
Figure 5.3	Interface area of SIMS sputtered crater showing the nanoscale porosity generated as the crater was sputtered on anodised Ti6Al4V substrate.....	55
Figure 5.4	Interface area of 75V Ti6Al4V anodised sample with Zirconia coating .....	56
Figure 5.5	C.P. Titanium SIMS Depth profile of Hydroxyapatite Coating ...	57
Figure 5.6	Depth Profile of Phosphorus in C.P. Titanium samples including anodised samples .....	58
Figure 5.7	Depth Profile of Calcium in C.P. Titanium samples including anodised samples.....	59
Figure 5.8	C.P. Titanium SIMS Depth profile of Zirconia Coating. ....	60
Figure 5.9	75 Volt anodised C.P. Titanium SIMS Depth profile of Zirconia Coating. ....	61
Figure 6.1	XRD diffractogram of CP titanium anodised samples (25-75V). ....	66
Figure 6.2	XRD diffractogram of CP titanium – 25V (red), 50V (BLACK), 75V (BLUE) anodised and hydroxyapatite coated .....	68
Figure 6.3	XRD Diffractogram of 25V C.P. Titanium Sample with Hydroxyapatite Coating.....	69
Figure 6.4	XRD Diffractogram of 50V C.P. Titanium Sample with Hydroxyapatite Coating.....	69
Figure 6.5	XRD Diffractogram of 75V C.P. Titanium Sample with Hydroxyapatite Coating.....	70
Figure 6.6	CP titanium diffractogram – 25V (red), 50V (BLACK), 75V (BLUE) anodised – Zirconia-coated samples. ....	71

Figure 6.7	Ti6Al4V Sample with Zirconia Sol gel Coating. ....	72
Figure 6.8	Ti6Al4V anodised at 25V Substrate with Zirconia Sol Gel Coating. ....	72
Figure 7.1	Contact angle of titanium samples .....	79
Figure 7.2	Surface Roughness of Titanium Samples measured using KLA Tencor Alpha-Step IQ Surface Profiler. ....	83
Figure 8.1	Micro-adhesion test sample.....	93
Figure 8.2	Micro-Adhesion Tester.....	94
Figure 8.3	Micro-adhesion test set-up showing the video attachment, monitor and measuring devices.....	95
Figure 8.4	Interface energy of Hydroxyapatite coatings on CP and Ti6Al4V Substrates.....	96
Figure 8.5	Interface energy of crack free Zirconia coatings on Titanium Substrates.....	97
Figure 8.6	Interface energy of (200nm) cracked Zirconia coatings on Titanium Substrates.....	97
Figure 8.7	Interface Toughness of Crack Free Zirconia coatings on Titanium Substrates.....	98
Figure 8.8	Interface Toughness of Cracked Zirconia coatings on Titanium Substrates.....	99
Figure 8.9	Interface Toughness of Hydroxyapatite coatings on Titanium Substrates.....	99
Figure 8.10	SEM micrograph of 25 Volt anodised C.P titanium sample with hydroxyapatite Coating after Micro-Adhesion Testing.....	101
Figure 8.11	SEM micrograph of 25 Volt anodised C.P titanium sample with hydroxyapatite Coating after Micro-Adhesion Testing.....	102
Figure 8.12	SEM micrograph of C.P titanium sample with hydroxyapatite Coating after Micro-Adhesion Testing.....	103
Figure 8.13	Shear stress of hydroxyapatite coatings on Titanium Substrates.....	104
Figure 8.14	Shear stress of Zirconia coatings on Titanium Substrates. ....	104
Figure 8.15	Shear stress of Thin Zirconia coatings on Titanium Substrates.....	105
Figure 8.16	Film Fracture Energy of Thin Zirconia coatings on Titanium Substrates .....	106

Figure 8.17	Film Fracture Energy of Zirconia coatings on Titanium Substrates .....	106
Figure 8.18	Film Fracture Energy of Hydroxyapatite coatings on Titanium Substrates .....	107
Figure 8.19	E Mod Nano-Indentation graph of Hydroxyapatite Sol Gel Coating .....	111
Figure 8.20	E Mod Nano-Indentation graph of Zirconia Sol Gel Coating ...	112
Figure 8.21	Hardness measurements in Nano-Indentation graph of Hydroxyapatite Coating.....	112
Figure 8.22	Hardness Measurements in Nano-Indentation graph of Zirconia Coating.....	113
Figure 9.1	Wear chart showing material loss after testing .....	121
Figure 9.2	C.P Titanium sample with cracked Zirconia coating. ....	124
Figure 9.3	75 volt anodised C.P Titanium sample with cracked Zirconia coating. ....	125

## APPENDIX

<b>Appendix-1</b>	25 Volt anodised C.P. Titanium zirconia coated depth profile. ....	145
<b>Appendix-2</b>	50 Volt anodised C.P. Titanium zirconia coated depth profile. ....	146
<b>Appendix-3</b>	Ti6AL4V- XRD Diffractogram of anodised samples involving 25, 50, 75 Volt plus Ti6Al4V sample. ....	147
<b>Appendix-4</b>	Ti6AL4V - XRD Diffractogram of 50V anodised sample with Zirconia Coating. ....	148
<b>Appendix-5</b>	Ti6AL4V - XRD Diffractogram of 75V anodised sample with Zirconia Coating. ....	148
<b>Appendix-6</b>	SEM of anodised 25 volt C.P. titanium sample after Micro-Adhesion Testing with Hydroxyapatite Sol Gel Coating 1K magnification. ....	149
<b>Appendix-7</b>	Nano-Indentation of anodised 25 volt C.P. titanium sample showing the E-Modulus. ....	150
<b>Appendix-8</b>	Nano-Indentation of anodised 50 volt C.P. titanium sample showing the E-Modulus. ....	151
<b>Appendix-9</b>	Nano-Indentation of anodised 75 volt C.P. titanium sample showing the E-Modulus. ....	152
<b>Appendix-10</b>	Nano-Indentation of anodised 25 volt C.P. titanium sample showing the Hardness Value. ....	153
<b>Appendix-11</b>	Nano-Indentation of anodised 50 volt C.P. titanium sample showing the Hardness Value. ....	154
<b>Appendix-12</b>	Nano-Indentation of anodised 75 volt C.P. titanium sample showing the Hardness Value. ....	155
<b>Appendix-13</b>	SEM of anodised 75 volt Ti6Al4V sample after Micro-Adhesion Testing with Hydroxyapatite Sol Gel Coating 40K magnification. ....	156
<b>Appendix-14</b>	SEM of anodised 75 volt Ti6Al4V sample after Micro-Adhesion Testing with Hydroxyapatite Sol Gel Coating 50K magnification. ....	157
<b>Appendix-15</b>	SEM of anodised 50 ti6Al4V sample after Micro-Adhesion Testing with Hydroxyapatite Sol Gel Coating 40K magnification. ....	158
<b>Appendix-16</b>	Micro adhesion results from testing and energy calculations .....	159



# LIST OF SYMBOLS, ABBREVIATIONS AND NOMENCLATURE

$V$	Volts
$A$	Constants
$B$	Constants
$\sigma_c$	Critical stress for cracking (MPa)
$\varepsilon_c$	Strain at first cracking
$E_f$	Young's Modulus of film (MPa)
$\sigma_r$	Residual Stress
$\lambda_f$	Fracture energy of film ( $\text{Jm}^{-2}$ )
$g(a)$	Constant
$a$	Dundas parameter
$K_{ic}$	Film toughness ( $\text{MPa.m}^{1/2}$ )
$d$	Oxide thickness
$\varepsilon$	Strain
$\sigma$	Stress (MPa)

## PUBLICATION LIST

**2007** R. Roest, A.J. Atanacio, B.A. Latella, R. Wuhrer, and B. Ben-Nissan, 'An Investigation of Sol gel coated zirconia thin films on anodised titanium substrate by secondary ion mass spectrometry and scanning electron microscopy' Materials Forum Volume 31- 2007. Edited by J.M. Cairney and S.P.Ringer

**2005** Roest, R. Heness, G., Latella, B., Ben-Nissan, B., "Fracture toughness of nanoscale Hydroxyapatite coatings on titanium substrates" Proc. 6th Int. Conf. Fract. & Strength of Solids, pp. 1297-1302, 2005

**2004** Roest, R., Heness, G., Latella, B. and Ben-Nissan, B. "Fracture toughness of nanoscale zirconia coatings on titanium substrates", Proc. Int. Conf. Structural Integrity and Fracture, pp. 325-330, 2004

**2004** R. Roest et al, "Adhesion of Sol-Gel Derived Zirconia Nano-Coatings on Surface Treated Titanium", *Key Engineering Materials*, Vols. 254-256, pp. 455-458, Trans Tech Publications, Switzerland. 2004.

**2004** Roest, R., Eberhardt, A.W., Latella, B., Wuhrer, R. & Ben-Nissan, B. 2004, 'Tribology and adhesion of zirconia nano-coatings on surface treated titanium', *Transactions - 7th World Biomaterials Congress, Transactions - 7th World Biomaterials Congress*, pp. 1783.-1787th 2004.

**2003** R. Roest et al, "Sol-Gel Derived Hydroxyapatite Coatings on Anodized Titanium Substrates", *XII International Workshop on Sol Gel Science and Technology*, pp. 112, 25-29 August 2003, Sydney.

**2001** R. Roest and B. Ben-Nissan, "Surface Modification of Anodized Titanium for Calcium Phosphate Coatings", *Proceedings of the Engineering Materials*, 23-26 September 2001, Melbourne. (Eds.) E. Pereloma and K. Raviprasad, pp. 115. 2001